PIGEON GENOMICS

Natural selection shaped the rise and fall of passenger pigeon genomic diversity

Gemma G. R. Murray,[1]* André E. R. Soares,[1]*† Ben J. Novak,[1,2] Nathan K. Schaefer,[3] James A. Cahill,[1] Allan J. Baker,[4]‡ John R. Demboski,[5] Andrew Doll,[5] Rute R. Da Fonseca,[6] Tara L. Fulton,[1,7] M. Thomas P. Gilbert,[6,8] Peter D. Heintzman,[1,9] Brandon Letts,[10] George McIntosh,[11] Brendan L. O'Connell,[3] Mark Peck,[5] Marie-Lorraine Pipes,[12] Edward S. Rice,[3] Kathryn M. Santos,[11] A. Gregory Sohrweide,[13] Samuel H. Vohr,[3] Russell B. Corbett-Detig,[3,14] Richard E. Green,[3,14] Beth Shapiro[1,14]§

The extinct passenger pigeon was once the most abundant bird in North America, and possibly the world. Although theory predicts that large populations will be more genetically diverse, passenger pigeon genetic diversity was surprisingly low. To investigate this disconnect, we analyzed 41 mitochondrial and 4 nuclear genomes from passenger pigeons and 2 genomes from band-tailed pigeons, which are passenger pigeons' closest living relatives. Passenger pigeons' large population size appears to have allowed for faster adaptive evolution and removal of harmful mutations, driving a huge loss in their neutral genetic diversity. These results demonstrate the effect that selection can have on a vertebrate genome and contradict results that suggested that population instability contributed to this species's surprisingly rapid extinction.

The passenger pigeon (*Ectopistes migratorius*) numbered between 3 billion and 5 billion individuals before its 19th-century decline and eventual extinction (*1*). Passenger pigeons were highly mobile and bred in large social colonies, and their population lacked clear geographic structure (*2*). Few vertebrates have populations this large and cohesive, and the neutral model of molecular evolution predicts that effective population size (N_e) and genetic diversity will increase in proportion to population size (*3*). Preliminary analyses of passenger pigeon genomes have, however, revealed surprisingly low genetic diversity (*4*). This finding has been interpreted within the framework of the neutral theory of molecular evolution as the result of a history of large demographic fluctuations (*4*). However, in large populations, natural selection may be particularly important in shaping genetic diversity: Population genetic theory predicts that selection will be more effective in large populations (*3*), and selection on one locus can cause a loss of diversity at other loci, particularly those that are closely linked (*5*–*8*). It has been suggested that this could explain why the genetic diversity of a species is poorly predicted by its population size (*9*–*11*).

We investigated the impact of natural selection on passenger pigeon genomes through comparative genomic analyses of both passenger pigeons and band-tailed pigeons (*Patagioenas fasciata*). Although ecologically and physiologically similar to passenger pigeons, band-tailed pigeons have a present-day population size three orders of magnitude smaller than that of their close relative, the passenger pigeon (*2*, *12*, *13*).

We applied a Bayesian skyline model of ancestral population dynamics to the mitochondrial genomes of 41 passenger pigeons from across their former breeding range (Fig. 1A and table S1) (*14*). This returned a most recent effective population size (N_e) of 13 million [95% highest posterior density (HPD) interval: 2 million to 58 million] and a similar, stable N_e for the previous 20,000 years (Fig. 1B). Although this N_e is much lower than the (census) population size (N_c), it is greater than previous estimates from analyses of nuclear genomes (*4*) and is likely to be conservative (*14*).

We compared nucleotide diversity (π) in the passenger pigeon nuclear genome to π in the band-tailed pigeon nuclear genome. We analyzed four high-coverage passenger pigeon genome assemblies (two newly sequenced and two from published raw data; table S2) and two high-coverage band-tailed pigeon genome assemblies. π was greater in passenger pigeons (average π = 0.008) than in band-tailed pigeons (average π = 0.004), but this difference is less than expected given their population sizes [it suggests that N_e/N_c was 0.0002 for passenger pigeons compared to 0.2 for band-tailed pigeons; (*14*)]. We estimated π for nonoverlapping 5-Mb windows across the genome and found that these species exhibit a correlated regional variation in π, but with greater variation in passenger pigeons (Fig. 2A and figs. S1 to S4).

To explore this variation, we mapped our scaffolds to the chicken genome assembly (*14*), which approximates chromosomal structure because karyotype and synteny are strongly conserved across birds (*15*). We found that low genetic diversity regions of the passenger pigeon genome are generally in the centers of macrochromosomes, whereas the edges of macrochromosomes and microchromosomes have higher diversity (Fig. 2B). Although this pattern is largely absent from the band-tailed pigeon genome, it is unlikely to be an artefact of ancient DNA damage as our assemblies had high coverage depth (table S2), we used conservative cut-offs for calling variants, and we recovered similar patterns after excluding variants more likely to have resulted from damage (fig. S5) (*14*). Instead, the pattern mirrors the recombination landscape of the bird genome, where recombination rates are lower in the centers of macrochromosomes, relative both to their edges and the microchromosomes (*14*, *15*).

We next investigated the impact of selection on the evolution of protein-coding regions of the genome in both species. We calculated the rate of adaptive substitution relative to the rate of neutral substitution (ω_a) and the ratio of nonsynonymous to synonymous polymorphism (*pN*/*pS*) for 5-Mb windows across the genome. A higher ω_a suggests stronger or more efficient positive selection, and a lower *pN*/*pS* suggests stronger or more efficient selective constraint. ω_a was higher (Mann-Whitney U test, $P = 1.3 \times 10^{-5}$) and *pN*/*pS* lower ($P = 8.2 \times 10^{-12}$) in passenger pigeons than band-tailed pigeons (Fig. 3 and fig. S6). We also found that ω_a was higher ($P = 2.2 \times 10^{-8}$) and *pN*/*pS* lower ($P = 4.1 \times 10^{-6}$) in high-diversity regions of the passenger pigeon genome compared to low-diversity regions (Fig. 3 and fig. S6). In addition, codon usage bias, which is thought to reflect selection for translational optimization (*16*), was greater in passenger pigeons than in band-tailed pigeons, and greater in high-diversity regions (figs. S19 and S20).

We also estimated the difference between the proportions of substitutions and polymorphisms that are nonsynonymous (the direction of selection, DoS) for individual genes, where a positive DoS indicates adaptive evolution. DoS was more often positive in passenger pigeons than in band-tailed pigeons and, in passenger pigeons, DoS was correlated with diversity (fig. S7). McDonald-Kreitman tests (*17*) identified 32 genes with evidence of adaptive evolution in passenger pigeons (table S3). Among them are genes associated with immune defense (e.g., *CPD*), seasonal consumption of high-sugar foods in passerine birds

[1]Department of Ecology and Evolutionary Biology, University of California, Santa Cruz, CA 95064, USA. [2]Revive & Restore, Sausalito, CA 94965, USA. [3]Department of Biomolecular Engineering, University of California Santa Cruz, Santa Cruz, CA 95064, USA. [4]Department of Natural History, Royal Ontario Museum, Toronto, ON M5S 2C6, Canada. [5]Department of Zoology, Denver Museum of Nature and Science, Denver, CO 80205, USA. [6]Centre for GeoGenetics, Natural History Museum of Denmark, University of Copenhagen, Øster Voldgade 5-7, 1350 Copenhagen, Denmark. [7]Environment and Climate Change Canada, 9250-49th Street, Edmonton, AB T6B 1K5, Canada. [8]NTNU University Museum, 7491 Trondheim, Norway. [9]Tromsø University Museum, UiT–The Arctic University of Norway, 9037 Tromsø, Norway. [10]Department of Biology, The Pennsylvania State University, University Park, PA 16802, USA. [11]Collections Department, Rochester Museum and Science Center, Rochester, NY 14607, USA. [12]Marie-Lorraine Pipes, Zooarchaeologist Consultant, Victor, NY 14564, USA. [13]A. Gregory Sohrweide D.D.S., Baldwinsville, NY 13027, USA. [14]University of California Santa Cruz Genomics Institute, 1156 High Street, Santa Cruz, CA 95064, USA.
*These authors contributed equally to this work. †Present address: Laboratório Nacional de Computação Científica, Petrópolis, RJ, Brazil. ‡Deceased
§Corresponding author. Email: beth.shapiro@gmail.com

Drastic population fluctuations explain the rapid extinction of the passenger pigeon

Chih-Ming Hung[a,1], Pei-Jen L. Shaner[a,1], Robert M. Zink[b], Wei-Chung Liu[c], Te-Chin Chu[d], Wen-San Huang[e,f,2], and Shou-Hsien Li[a,2]

[a]Department of Life Science and [d]Department of Computer Science and Information Engineering, National Taiwan Normal University, Taipei 116, Taiwan; [b]Department of Ecology, Evolution, and Behavior, and Bell Museum, University of Minnesota, St. Paul, MN 55108; [c]Institute of Statistical Science, Academia Sinica, Taipei 11529, Taiwan; [e]Department of Biology, National Museum of Natural Science, Taichung 404, Taiwan; and [f]Department of Life Sciences, National Chung Hsing University, Taichung 402, Taiwan

Edited by Wen-Hsiung Li, University of Chicago, Chicago, IL, and approved May 27, 2014 (received for review January 24, 2014)

To assess the role of human disturbances in species' extinction requires an understanding of the species population history before human impact. The passenger pigeon was once the most abundant bird in the world, with a population size estimated at 3–5 billion in the 1800s; its abrupt extinction in 1914 raises the question of how such an abundant bird could have been driven to extinction in mere decades. Although human exploitation is often blamed, the role of natural population dynamics in the passenger pigeon's extinction remains unexplored. Applying high-throughput sequencing technologies to obtain sequences from most of the genome, we calculated that the passenger pigeon's effective population size throughout the last million years was persistently about 1/10,000 of the 1800's estimated number of individuals, a ratio 1,000-times lower than typically found. This result suggests that the passenger pigeon was not always super abundant but experienced dramatic population fluctuations, resembling those of an "outbreak" species. Ecological niche models supported inference of drastic changes in the extent of its breeding range over the last glacial–interglacial cycle. An estimate of acorn-based carrying capacity during the past 21,000 y showed great year-to-year variations. Based on our results, we hypothesize that ecological conditions that dramatically reduced population size under natural conditions could have interacted with human exploitation in causing the passenger pigeon's rapid demise. Our study illustrates that even species as abundant as the passenger pigeon can be vulnerable to human threats if they are subject to dramatic population fluctuations, and provides a new perspective on the greatest human-caused extinction in recorded history.

genome sequences | ancient DNA | toe pad

Rare species with restricted geographic distributions are more likely to go extinct than abundant, widespread species because the former are more vulnerable to environmental stochasticity, diseases, and human disturbances (1). Therefore, the extinction risk of common species tends to be ignored. As a result, factors responsible for the extinction of once abundant species, whose demise could impact ecosystems profoundly, are not well understood. A species with dramatic population cycles could be especially vulnerable to extinction when it becomes rare (2, 3), and large-scale population fluctuations could increase extinction risk (4). Hence, knowledge of long-term demographic history allows a better perspective on a species' extinction risk than a snapshot of population size (4, 5).

Applying population genetic analysis to ancient DNA (aDNA) extracted from the remains of extinct species can improve our understanding of the species' history and potential reasons for its extinction (6). Estimating extinct species' demographic history is, however, often difficult because specimens are scarce and the quality of remaining DNA is poor (7). By adapting high-throughput sequencing technologies, we obtained high-quality genome sequences for the passenger pigeon (*Ectopistes migratorius*), which went extinct 100 y ago. These sequences allowed us to estimate the long-term population history in unprecedented detail and to provide a novel hypothesis as to why the most abundant bird the world had known became extinct so rapidly.

Migratory flocks of the passenger pigeon were once so immense that they were said to have blanketed the skies of eastern North America (8). In one of many illustrative descriptions, John James Audubon recounted a mile-wide flock of migrating passenger pigeons that passed overhead, blocking the sun for 3 consecutive days (9). The vast numbers of passenger pigeons have led ecologists to suggest that this bird was a keystone species in North American ecosystems (10, 11). This pigeon is believed to have influenced forest composition by consuming and dispersing acorns, beechnuts, and other mast crops on which it fed (10, 11), disrupted local communities, out-competed other mast-eating species, damaged trees by the weight of large flocks leading to breaking of large limbs of trees, and killed surface vegetation with thick layers of excrement (8, 11).

Although the passenger pigeon population was estimated at 3–5 billion individuals in the early and middle 1800s, the last passenger pigeon died at the Cincinnati Zoo on September 1, 1914 (8). The extinction of this abundant bird in a mere five decades is a poignant reminder that even a bird numbering in

Significance

The number of passenger pigeons went from billions to zero in mere decades, in contrast to conventional wisdom that enormous population size provides a buffer against extinction. Our understanding of the passenger pigeon's extinction, however, has been limited by a lack of knowledge of its long-term population history. Here we use both genomic and ecological analyses to show that the passenger pigeon was not always super abundant, but experienced dramatic population fluctuations, which could increase its vulnerability to human exploitation. Our study demonstrates that high-throughput–based ancient DNA analyses combined with ecological niche modeling can provide evidence allowing us to assess factors that led to the surprisingly rapid demise of the passenger pigeon.

Author contributions: C.-M.H., P.-J.L.S., R.M.Z., and S.-H.L. designed research; C.-M.H., P.-J.L.S., R.M.Z., and S.-H.L. performed research; W.-S.H. and S.-H.L. contributed new reagents/analytic tools; C.-M.H., P.-J.L.S., W.-C.L., and T.-C.C. analyzed data; and C.-M.H., P.-J.L.S., R.M.Z., W.-S.H., and S.-H.L. wrote the paper.

The authors declare no conflict of interest.

This article is a PNAS Direct Submission.

Data deposition: The sequences reported in this paper have been deposited in the GenBank database (accession no. SRP042357).

See Commentary on page 10400.

[1]C.-M.H. and P.-J.L.S. contributed equally to this work.

[2]To whom correspondence may be addressed. E-mail: wshuang@mail.nmns.edu.tw or t43028@ntnu.edu.tw.

This article contains supporting information online at www.pnas.org/lookup/suppl/doi:10.1073/pnas.1401526111/-/DCSupplemental.

dynamics of dissolved nutrient patches. We have yet to identify the frequency of occurrence and magnitude spectra of such patches in specific microbial food webs. They undoubtedly represent interesting ecological niches for bacteria, and they will also contribute much to our understanding of the flow of nutrients and energy in aquatic ecosystems if they prove to be major pathways.

References and notes

1. J. C. Goldman, *Bull. Mar. Sci.* **35**, 462 (1984).
2. E. M. Purcell, *Am. J. Phys.* **45**, 3 (1977).
3. G. A. Jackson, *Limnol. Oceanogr.* **32**, 1253 (1987).
4. W. Bell and R. Mitchell, *Biol. Bull.* **143**, 265 (1972).
5. J. G. Mitchell, A. Okubo, J. A. Fuhrman, *Nature* **316**, 58 (1985); J. D. Bowen, K. D. Stolzenbach, S. W. Chisholm, *Limnol. Oceanogr.* **38**, 36 (1993).
6. N. Blackburn, unpublished observations.
7. _____, F. Azam, Å. Hagström, *Limnol. Oceanogr.* **42**, 613 (1997).
8. Samples were taken, immediately before observation, from the vicinity of algal mats in a large seawater aquarium with high through-flow. The microbial community could be characterized as being rich and diverse. Identical communities have been observed in completely natural habitats. A standard microscope fitted with a dark-field condenser was used for observation with a 10× objective giving a depth of field of ~20 μm. The magnification was increased for some recordings with a magnifying lens. Samples were observed in a chamber made by a 1.5-mm-thick rubber O-ring placed on top of a microscope slide and covered with a cover slip. A fiber optic light source was used for illumination to minimize heat transfer. A standard video camera and VCR were used for recordings.
9. A. Andersson, C. Lee, F. Azam, Å. Hagström, *Mar. Ecol. Prog. Ser.* **23**, 99 (1985); P. A. Jumars, D. L. Penry, J. A. Baross, M. J. Perry, B. W. Frost, *Deep-Sea Res.* **36**, 483 (1989).
10. J. T. Lehman and D. Scavia, *Proc. Natl. Acad. Sci. U.S.A.* **79**, 5001 (1982).
11. P. J. L. Williams and L. R. Muir, in *Ecohydrodynamics*, J. C. J. Nihoul, Ed. (Elsevier, New York, 1981), pp. 209–218; D. J. Currie, *J. Plankton Res.* **6**, 591 (1984); G. A. Jackson, *Nature* **284**, 439 (1980).
12. D. A. Brown and H. C. Berg, *Proc. Natl. Acad. Sci. U.S.A.* **71**, 1388 (1974).
13. T. Fenchel, *Microbiology* **140**, 3109 (1994); J. G. Mitchell *et al.*, *Appl. Environ. Microbiol.* **61**, 877 (1995); J. G. Mitchell, L. Pearson, S. Dillon, K. Kantalis, *ibid.*, p. 4436; J. G. Mitchell, L. Pearson, S. Dillon, *ibid.* **62**, 3716 (1996); G. M. Barbara and J. G. Mitchell, *ibid.*, p. 3985.
14. Samples of seawater were enriched with 0.02% tryptic soy broth and left overnight, after which the culture contained strains of highly motile bacteria. Samples were sandwiched between a slide and cover slip after the addition of cells from a pure culture of *Pavlova lutheri*. A ring of bacteria around the air-water interface of the chamber indicated near anoxia inside the chamber.
15. P. A. Wheeler, in *Nitrogen in the Marine Environment*, E. J. Carpenter and D. G. Capone, Eds. (Academic Press, New York, 1983), p. 309.
16. F. Azam and J. W. Ammerman, in *Flows of Energy and Materials in Marine Ecosystems*, M. J. R. Fasham, Ed. (Plenum, New York, 1984), p. 345.
17. N. Blackburn, T. Fenchel, J. Mitchell, data not shown.
18. J. D. Bowen and K. D. Stolzenbach, *J. Fluid Mech.* **236**, 95 (1992).
19. L. Karp-Boss, E. Boss, P. A. Jumars, *Oceanogr. Mar. Biol. Annu. Rev.* **34**, 71 (1996).
20. H. C. Berg and D. A. Brown, *Nature* **239**, 500 (1972).
21. Video sequences were digitized to computer memory at 25 frames s^{-1}. The resulting digital film-strips were analyzed frame by frame for trajectories of movement by LabTrack (DiMedia, Kvistgaard, Denmark). Objects moving out of the plane of focus resulted in short tracks and were filtered out of the set of track vectors. Tumbles were detected at points where changes in trajectory angle between two video frames exceeded 1 rad. Runs were defined as periods between tumbles.
22. The enteric bacterium *E. coli* swims in straight runs interspersed by tumbles (*20*). Positive taxis is achieved by lengthening runs when positive changes in concentration are detected over a period of time (*12*). The model refined by Brown and Berg states that the mean increase in run duration $\Delta\tau$ is proportional to the positive rate of change of attractant concentration

$$\Delta\tau = \frac{\alpha}{K_D}\frac{\partial C}{\partial t}$$

where C is concentration, K_D is a dissociation constant (100 μM), and α is a sensitivity constant (1000 s). Simulations were performed by allowing cells to move against a concentration field (*3*). Cells were moved a distance determined by their swimming velocity and heading angle from a physical location whose attractant concentration was C_1 to another location of concentration C_2, within each simulated time step dt. The change in mean run duration could thus be calculated as

$$\Delta\tau = \frac{\alpha}{K_D}\frac{C_2 - C_1}{dt}$$

Negative changes were ignored. Run durations are Poisson distributed (*12*). The probability of tumbling after each time step is $dt/(\tau + \Delta\tau)$. The desired Poisson process was implemented with a random generator to decide whether or not to tumble after each time step. Tumbles were simulated as reversals, and a Brownian rotation of 1 rad s^{-1} was introduced. Swimming velocities and mean run durations were acquired from tracks of live cells.
23. The steady-state concentration field $C(r)$ was calculated as

$$C(r) = \frac{E}{4\pi D\sqrt{r}}$$

where oxygen exudation rate $E = 0.25$ fmol s^{-1} was estimated from light-saturated photosynthesis of a cell 4 μm in diameter. The diffusion coefficient $D = 10^{-5}$ cm^2 s^{-1}. The inverse square-root dependency on the distance r from the source was introduced instead of inverse proportionality (*3*) to more closely approximate its shape in the flat chamber.
24. The concentration field $C(r,t)$ of a spreading patch was calculated as

$$C(r,t) = M(4\pi rDt)^{-1.5}e^{-\frac{r^2}{4Dt}}$$

where M is the amount of matter released (1 pmol), and $D = 10^{-5}$ cm^2 s^{-1}. Simulations were based on 100 individuals initially distributed randomly within a radius of 1 mm from the source. Velocity $v = 50$ μm s^{-1}, $\tau = 0.4$ s.
25. The mass flow of a solute at concentration C with diffusion coefficient D toward a sphere of radius a is $4\pi aDC$.

26. We thank the Swedish Foundation for International Cooperation in Research and Higher Education (STINT), the Danish National Research Council (SNF), the Australian Research Council, and Flinders University for support of this study.

12 June 1998; accepted 3 November 1998

Prevention of Population Cycles by Parasite Removal

Peter J. Hudson,* Andy P. Dobson, Dave Newborn

The regular cyclic fluctuations in vertebrate numbers have intrigued scientists for more than 70 years, and yet the cause of such cycles has not been clearly demonstrated. Red grouse populations in Britain exhibit cyclic fluctuations in abundance, with periodic crashes. The hypothesis that these fluctuations are caused by the impact of a nematode parasite on host fecundity was tested by experimentally reducing parasite burdens in grouse. Treatment of the grouse population prevented population crashes, demonstrating that parasites were the cause of the cyclic fluctuations.

Mathematical models have shown that a density-dependent response acting with a time delay can generate population cycles between natural enemies and their prey (*1*). Indeed, trophic interactions rather than intrinsic mechanisms are now considered by many to be the principal cause of cycles in microtine rodents (*2*), snowshoe hares (*3*), and red grouse (*4*). The definitive test of these hypotheses is to stop population cycles by manipulating the causative mechanism. Here, we report on a long-term, large-scale, replicated field experiment that examined the capacity of parasites to cause cycles. The impact of the parasitic nematode *Trichostrongylus tenuis* on individual red grouse (*Lagopus lagopus scoticus*) was reduced through the application of an anthelmintic before a cyclic population crash in northern England.

Extensive investigations of hunting records from 175 individually managed grouse populations, coupled with detailed intensive demographic studies, have shown that 77% of red grouse populations exhibit significant cyclic fluctuations with a period between 4 and 8 years (Fig. 1A) (*4*). Population growth rate is negatively related to the intensity of worm infection in adult grouse (Fig. 1B), and poor breeding production is correlated with worm intensity (Fig. 1C), so that population crashes are associated with high parasite intensities. Analyses of parasite-host models predict that parasitic helminths can cause population cycles when they induce a reduction in host fecundity

P. J. Hudson, Institute of Biological Sciences, University of Stirling, Stirling FK9 4LA, UK. A. P. Dobson, Department of Ecology and Evolutionary Biology, Eno Hall, Princeton University, Princeton, NJ 08544–1003, USA. D. Newborn, Game Conservancy Trust, Swaledale, North Yorkshire DL8 3HG, UK.

*To whom correspondence should be addressed. E-mail: p.j.hudson@stir.ac.uk

Parasites and climate synchronize red grouse populations

Isabella M. Cattadori[1], Daniel T. Haydon[2] & Peter J. Hudson[1]

[1]*Center for Infectious Diseases Dynamics, Mueller Laboratory, The Pennsylvania State University, University Park, Pennsylvania 16802, USA*
[2]*Division of Environmental and Evolutionary Biology, University of Glasgow, Glasgow G12 8QQ, UK*

There is circumstantial evidence that correlated climatic conditions can drive animal populations into synchronous fluctuations in abundance[1–5]. However, it is unclear whether climate directly affects the survival and fecundity of individuals, or indirectly, by influencing food and natural enemies. Here we propose that climate affects trophic interactions and could be an important mechanism for synchronizing spatially distributed populations. We show that in specific years the size of red grouse populations in northern England either increases or decreases in synchrony. In these years, widespread and correlated climatic conditions during May and July affect populations regionally and influence the density-dependent transmission of the gastrointestinal nematode *Trichostrongylus tenuis*, a parasite that reduces grouse fecundity[6]. This in turn forces grouse populations into synchrony. We conclude that specific climatic events may lead to outbreaks of infectious diseases or pests that may cause dramatic, synchronized changes in the abundance of their hosts.

Nonlinear interactions between climate and population size can influence not only temporal changes in abundance but can also lead to spatial synchrony at a range of scales[1–5,7,8]. About 50 years ago, Moran[9] proposed that uncoupled populations with identical linear density-dependent structure will asymptotically synchronize in phase under the influence of correlated environmental perturbations, and the correlation between populations will equal the correlation between the extrinsic factors. Since Moran suggested his theorem, researchers have looked for evidence of the 'Moran effect' across animal taxa and investigated how environmental noise interacts with nonlinear population dynamics, the 'nonlinear Moran effect'[2,8,10]. However, researchers have yet to identify the underlying process that generates correlated fluctuations between populations in any natural system. In populations in which fluctuations are driven by a trophic interaction, such as predator—prey, host–parasitoid or host–parasite interactions, the correlated climatic effects may operate either on these density-dependent mechanisms or more directly on population abundance, and thus move populations into a synchronous phase. Here we examine this hypothesis in the natural system of the red grouse (*Lagopus lagopus scoticus*) and its gastrointestinal parasite *Trichostrongylus tenuis*, a nematode known to play a major role in reducing fecundity and destabilizing grouse populations[6,11,12].

We used 91 time series of annual red grouse harvesting data obtained from managed grouse moors in northern England between 1839 and 1994 and collected by The Game Conservancy Trust (Fig. 1). Red grouse harvest data have proved to be a fair reflection of spatio-temporal changes in population density and annual productivity[13]. The majority (59%) of these time series exhibit cyclic fluctuations with an average period of 7 years (range 3–13 years)[14,15]. Each grouse population is embedded within one of five discrete regions of contiguous habitat[15] and we analysed synchrony between populations in each of these regions. Common statistical techniques can be used to identify spatial synchrony[16] and provide an estimate of average synchrony between time series, but they fail to identify the years in which time series are forced into synchrony. To achieve this, the dynamical state of each red grouse population was represented in a state-based Markov chain model that described temporal transitions between four phase states based on three consecutive years of observations: a cycle trough, a consecutive increase, a cycle peak and a consecutive decrease. For each region, we examined changes in the annual proportion of populations in each state, which allowed us to identify the years in which populations were forced into significant state-synchrony and quantify the state that these populations converge onto, in these years[17]. As an annual index of state synchrony among populations within each of the five regions, we applied the Shannon–Weaver diversity index to the proportion of populations in each state[17]. Populations were considered to be in synchrony when the diversity index deviated below the lower 95% confidence interval predicted by the Markov state transition model under the null hypothesis of no coupling between populations. Hence, a synchronous year can arise either as a dynamically predictable episode, as a consequence of synchrony in the preceding year, or as an unpredicted 'collective forcing episode' (CFE) that brings previously asynchronous populations into the same synchronous state[8,10]. To identify years when these forcing events occurred, we calculated whether the diversity index fell outside the one-step 95% confidence interval, conditional on the state configuration in the previous year[17]. We focused our analyses on the years in which these forcing events occurred and looked for the putative synchronizing mechanism.

The diversity index calculated among populations within each of the five regions revealed that no regular pattern characterized the incidence of the forcing episodes (Fig. 2a). The majority of populations converged on a common dynamical state: 'upward' CFEs—either two successive years of increased abundance (32% of CFEs) or peaks (32% of CFEs)—or, less frequently, 'downward' CFEs—when populations converged on two successive years of population decline (8% of CFEs) or a trough (28% of CFEs) (Fig. 2b). On the basis of knowledge of the red grouse system, we propose that there are two major demographic circumstances that would tend to generate such collective forcing episodes in these harvesting data:

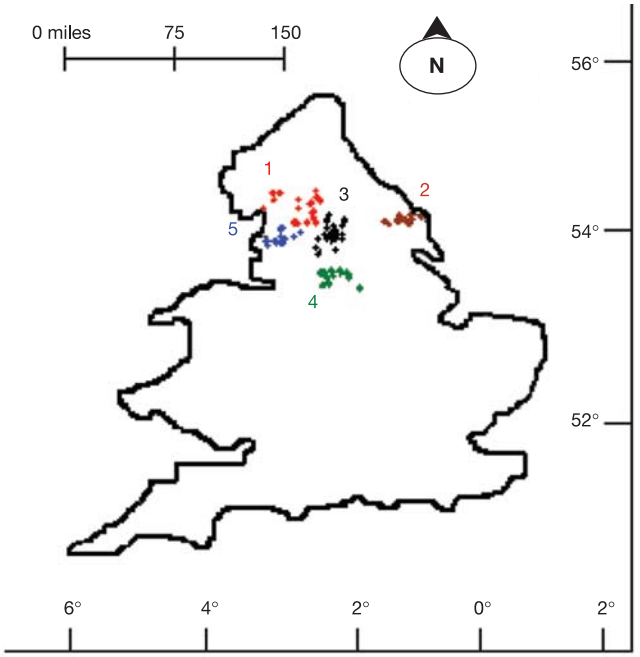

Figure 1 Locations of the 91 red grouse populations that provided annual harvesting records between 1839 and 1994. Populations were aggregated into five geographically distinct regions of contiguous grouse habitat (heather-dominant moorland), each represented here by a different colour. Synchrony between populations was examined within each of these distinct regions.